Electron Emission Models for Simulation

K. L. Jensen

U.S. NAVAL RESEARCH LABORATORY

Code 6362, MSTD, NRL, Washington DC

P^3 WORKSHOP 2021
November 10-12, 2021

We gratefully acknowledge:
(NRL), A. Shabaev, M. Osofsky, S. Lambrakos; (USNA) D. Finkenstadt;
(Leidos) J. Petillo; (AFRL) J. Riga, D. Shiffler; (ASU) O. Chubenko;
(LANL) D. Dimitrov, N. Moody, A. Neukirch, J. Smedley, S. Tretiak

Further Information

This presentation is drawn from cleared open sources:

1. K.L. Jensen, J.L. Lebowitz, J.M. Riga, D.A. Shiffler, and R. Seviour, “Reevaluating the Hartman Effect for Field Emission” (*submitted*, Sept. 2021)
2. K. L. Jensen, A. R. Shabaev, M. Osofsky, “Theory and Modeling of Ultrafast Electron Emission from Nanostructures”, *NRL Memorandum Report* IR-6362-21-34-U, (September 30, 2021)
3. K.L. Jensen, J.L. Lebowitz, J.M. Riga, D.A. Shiffler, and R. Seviour, “Wigner wave packets: Transmission, reflection, and tunneling”, Phys. Rev. B **103**155427 (2021). 10.1103/PhysRevB.103.155427
4. K.L. Jensen, A. Shabaev, S.G. Lambrakos, D. Finkenstadt, N.A. Moody, A.J. Neukirch, S. Tretiak, D.A. Shiffler, and J.J. Petillo, “Analytic model of electron transport through and over non-linear barriers”, J. Appl. Phys. **127(23)**, 235301 (2020). 10.1063/5.0009759
5. K.L. Jensen, A. Shabaev, S.G. Lambrakos, D. Finkenstadt, J.J. Petillo, A.M. Alexander, J. Smedley, N.A. Moody, H. Yamaguchi, F. Liu, A.J. Neukirch, and S. Tretiak, “An extended moments model of quantum efficiency for metals and semiconductors”, J. Appl. Phys. **128(1)**, 015301 (2020). 10.1063/5.0011145

Additional Supportive Sources:

6. N.A. Moody, K.L. Jensen, A. Shabaev, S.G. Lambrakos, J. Smedley, D. Finkenstadt, J.M. Pietryga, P.M. Anisimov, V. Pavlenko, E.R. Batista, J.W. Lewellen, F. Liu, G. Gupta, A. Mohite, H. Yamaguchi, M.A. Hoffbauer, and I. Robel, “Perspectives on Designer Photocathodes for X-ray Free-Electron Lasers: Influencing Emission Properties with Heterostructures and Nanoengineered Electronic States”, Physical Review Applied **10(4)**, 047002 (2018). PhysRevApplied.10.047002
7. Jensen2019b K.L. Jensen, M. McDonald, O. Chubenko, J.R. Harris, D.A. Shiffler, N.A. Moody, J.J. Petillo, and A.J. Jensen, “Thermal-field and photoemission from meso- and micro-scale features: Effects of screening and roughness on characterization and simulation”, J. Appl. Phys. **125(23)**, 234303 / 1-25 (2019). 10.1063/1.5097149
8. K.L. Jensen, M. McDonald, J.R. Harris, D.A. Shiffler, M. Cahay, and J.J. Petillo, “Analytic model of a compound thermal-field emitter and its performance”, J. Appl. Phys. **126(24)**, 245301 (2019). 10.1063/1.5132561
9. K.L. Jensen, “A reformulated general thermal-field emission equation”, J. Appl. Phys. **126(6)**, 065302 / 1-13 (2019). 10.1063/1.5109676
10. K.L. Jensen, D. Finkenstadt, D.A. Shiffler, A. Shabaev, S.G. Lambrakos, N.A. Moody, and J.J. Petillo, “Analytical Models of Transmission Probabilities for Electron Sources”, J. Appl. Phys. **123(6)**, 065301 (2018). doi.org/10.1063/1.5018602

SPEED
Canonical emission equations
Analytic Methods
Smooth Surface
Isolated Emitter
Instantaneous Emission

Buridan's PICass

ACCURACY
Space Charge + Curvature Barriers
Adaptive Meshing
Intrinsic Emittance
Shielding
Delayed Emission & Transit Times

- Canonical Eqs. (FD, FN, RLD) are fast, but neglect Photo-Thermal-Field & mesoscale; analytical models are exact but actual emitters are complicated; instantaneous emission assumed
- PIC handles Shielding, Space Charge, and Field affected by roughness, but nanoscale primary determinant of all thermal-field-photoemission contributions

Thermal-Field-Photoemission Emission Challenges to Simulation Codes:

Everything affects emission. Emission affects T and surface field.
Space charge, T, F affects Everything

Absorption-Transport-Emission Model

$$QE = [1 - R(\omega)] \frac{\int_{E_a}^{\hbar\omega - E_g} EdE \int_{\sqrt{E_a/E}}^{1} xdx\, D_{\Delta}(Ex^2)\, f_{\lambda}(x, E)}{2\int_0^{\hbar\omega - E_g} E\left[\int_0^1 dx\right] dE} \qquad (1)$$

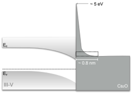

High, thin triangular barrier: $s^2 \equiv (\hbar\omega - E_g - E_a)/E_a$ and $C \approx n(1 - R)/(1 + p)$ with $n = O(1)$

$$D_{\Delta}(E) \approx \frac{4[E(E - E_a)]^{1/2}}{(E^{1/2} + (E - E_a)^{1/2})^2} \rightarrow QE \approx \frac{2Cs^5}{(1 + s^2)(1 + \sqrt{1 + s^2})(s + \sqrt{1 + s^2})} \qquad (2)$$

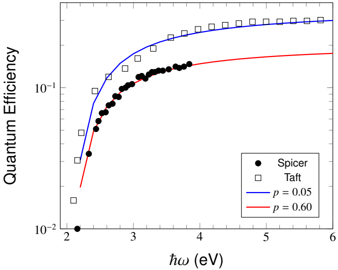

Cs_3Sb: $E_g = 1.6$ eV, $E_a = 0.4$ eV, $R = 0.2$

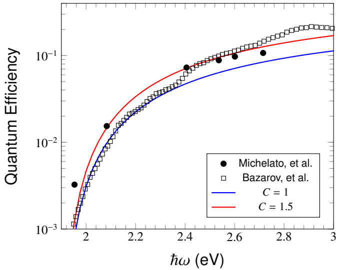

K_2CsSb: $E_g = 1.2$ eV, $E_a = 0.7$ eV, $R = 0.2$

See Ref. 6

Drude-Lorentz Model

- Laser penetration depth $\delta(\omega)$ and reflectivity $R(\omega)$

$$R(\omega) = \frac{(n-1)^2 + k^2}{(n+1)^2 + k^2}$$
$$\delta(\omega) = \frac{c}{2k\omega} \qquad (3)$$

n and k from Bound (Lorentz) $\hat{\varepsilon}_b$ & free (Drude) $\hat{\varepsilon}_f$ components $\Rightarrow (f_j, \Gamma_j, \omega_j)$

$$\hat{\varepsilon}(\omega) = \varepsilon_0 \left(n^2 - k^2 + 2ink\right)$$
$$\equiv \hat{\varepsilon}_f + \hat{\varepsilon}_b$$
$$\hat{\varepsilon}_f(\omega) = 1 - \frac{f_0\ \omega_p^2}{\omega(\omega + i\ \Gamma_0)} \qquad (4)$$
$$\hat{\varepsilon}_b(\omega) = \sum_{j=1}^{n} \frac{f_j\ \omega_p^2}{(\omega_j^2 - \omega^2 - i\omega\Gamma_j)}$$

- Right: Perovskites; metals, Multialkali antimonides = similar results

See Ref. 5

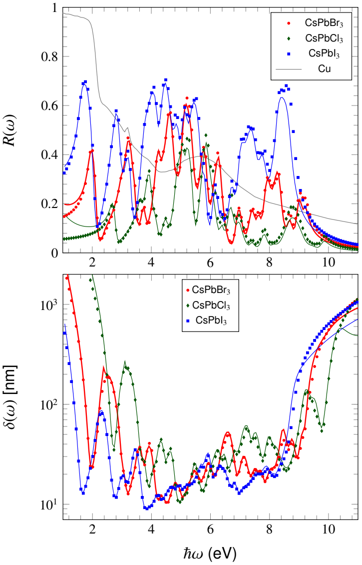

The Canonical Equations

Thermal : Richardson-Laue-Dushman

C. Herring, M. Nichols, Rev. Mod. Phys. 21, 185 (1949).

$$J_{RLD}\left(T\right) = A_{RLD} T^2 \exp\left(-\frac{\phi}{k_B T}\right) \quad (5)$$

Field : Fowler Nordheim

E.L. Murphy, R.H. Good, Phys Rev 102, 1464 (1956).

$$J_{FN}\left(F\right) = \frac{A_{FN}}{t(y)^2} F^2 \exp\left(-v(y)\frac{B_{FN}\Phi^{3/2}}{F}\right) \quad (6)$$

Photo : Fowler-DuBridge

L.A. DuBridge, Phys. Rev. 43, 0727 (1933).

$$QE \equiv \frac{\hbar\omega}{q}\left(\frac{J}{I_\omega}\right) \propto \left(\hbar\omega - \phi\right)^2 \quad (7)$$

Secondary : Baroody

E.M. Baroody, Phys. Rev. **78**, 780 (1950)

$$\delta(E_o) = BE_o e^{-\lambda} \int_0^1 \exp\left(\lambda s^2\right) ds \quad (8)$$

Space Charge : Child-Langmuir

I. Langmuir, Phys. Rev. **2**, 450 (1913).

$$J_{CL}\left(\varphi_a\right) = \frac{4\varepsilon_0}{9D^2}\left(\frac{2q}{m}\right)^{1/2} \varphi_a^{3/2} \quad (9)$$

Φ = Work Function; T = Temperature; $F = q\mathcal{E}$;
$\hbar\omega$ = Photon energy; I_ω = laser intensity;
E_o = Primary electron beam energy;
λ = energy loss per unit length
D = anode-cathode gap; φ_a = anode potential

Equations follow from J evaluation

Shape Factor Method

$\sigma(E)$ and $u(E)$ (related to $\partial_E \theta$) defined by

$$\sigma(E) = \int_{x_-}^{x_+} \left\{ \frac{U(x) - E}{U_o - E} \right\}^{1/2} \frac{dx}{L} \qquad (10)$$

$$u(E) = \int_{x_-}^{x_+} \left\{ \frac{U_o - E}{U(x) - E} \right\}^{1/2} \frac{dx}{L} \qquad (11)$$

Length/Height scales: ($\phi = \Phi - \sqrt{4QF}$)

$$\begin{aligned} FL(E) &= \sqrt{(\mu + \Phi - E)^2 - 4QF} \\ \hbar\kappa(E) &\equiv \sqrt{2m(\mu + \phi - E)} \end{aligned} \qquad (12)$$

Gamow factor using Shape Function

$$\theta(E) = 2\,\sigma(E)\,\kappa(E) L(E) \qquad (13)$$

$\sigma(E)$ is factor accounting for shape

- rectangular: $\sigma_{\square} = 1$
- triangular: $\sigma_{\triangle} = 2/3 = 0.6667$
- parabolic: $\sigma_{\cap} = \pi/4 = 0.7854$

$\sigma(E)$ = red / blue; $\mu = 7$ eV, $\Phi = 2$ eV, $F = 1$ eV/nm

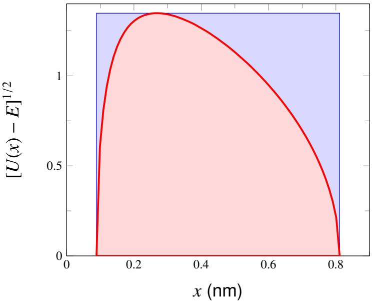

- Relation to Fowler-Nordheim Equation

$$J_{FN}(F, \Phi) = \frac{qm}{2\pi^2\hbar^3} \frac{e^{-2\sigma[y(\mu)]\kappa(\mu)L(\mu)}}{[2u(\mu)\kappa(\mu)L(\mu)]^2}$$

- Relation to SN Functions, $y = \sqrt{4QF}/\Phi$

$$\sigma(\mu) = \frac{2v(y)}{3(1-y)\sqrt{1+y}}; \quad u(\mu) = \frac{2t(y)}{\sqrt{1+y}}$$

General Current Density Relation I

$$J(F,T) = \int dJ(E) = \frac{qm}{2\pi^2 \beta_T \hbar^2} \int_0^\infty h(E) \frac{\ln\{1+\exp[\beta_T(\mu - E)]\}}{1 + C(E)\exp[\theta(E)]} dE \tag{14}$$

- $\triangle$ Gamow and Field E Slope Factor

$$\theta(E) \equiv \frac{4}{3}\kappa(E)L(E) = \frac{4\sqrt{2m}}{3\hbar}(V_o - E)^{3/2} \tag{15}$$

$$\beta_F(E) \equiv -\frac{d\theta}{dE} = \frac{2\sqrt{2m}}{\hbar F}(V_o - E)^{1/2} \tag{16}$$

- Linearize (E_m is location of maximum):

$$\theta(E) = \theta(E_m) - \beta_F(E_m)[E_m - E] \tag{17}$$

- Thermal E Slope factor: $\beta_T \equiv 1/k_B T$

Triangular (FN) Barrier: $V_o = \mu + \Phi$

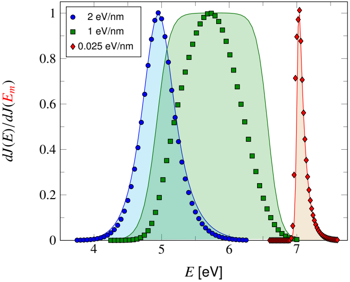

$V(x) = V_o - Fx$
dJ (normalized) for $\mu = 5$ eV, $\Phi = 2$ eV
$T = 1000$ K for different F.
Symbols are Exact, Lines are linearized θ;
color areas: integrand of Eq. (14) using Eq. (17).

General Current Density Relation II

The reason for replacing $\theta(E)$ by its linear approximation $\theta(E_m) - \beta_F(E_m)(E - E_m)$ is because doing so leads to an analytic General Thermal-Field-Photoemission equation

GTF in linear θ Approximation (h = C = 1)

$$
\begin{aligned}
J(F,T) &\approx A_{RLD} T^2 N(n,s) \\
n(F,T) &\equiv \frac{\beta_T}{\beta_F(E_m)} \\
s(F,T) &\equiv \theta(E_m) + \beta_F(E_m)(E_m - E)
\end{aligned}
\qquad (18)
$$

- N has field, thermal dominated parts

$$
\begin{aligned}
N(n,s) &\approx e^{-s} n^2 \Sigma\left(\frac{1}{n}\right) + e^{-ns}\Sigma(n) \\
\Sigma(x) &\approx \frac{1+x^2}{1-x^2} - 0.36\, x^2 - \ldots
\end{aligned}
\qquad (19)
$$

- $\Sigma(x)$ is singular at $x = 1$: both T and F components required to cancel it out
- field limit is FN; thermal limit is RLD

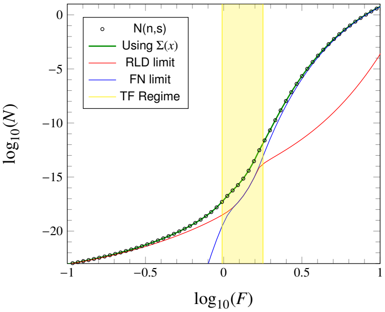

Photoemission: (h,C are involved)

$$
J_P \propto (\hbar\omega - \phi)^2 + \frac{\pi^2}{3}\left(\beta_T^{-2} + \beta_F^{-2}\right) \qquad (20)
$$

$$
(n^2 \ll 1, J_P \rightarrow J_{FD})
$$

Quadratic and MIM Barriers

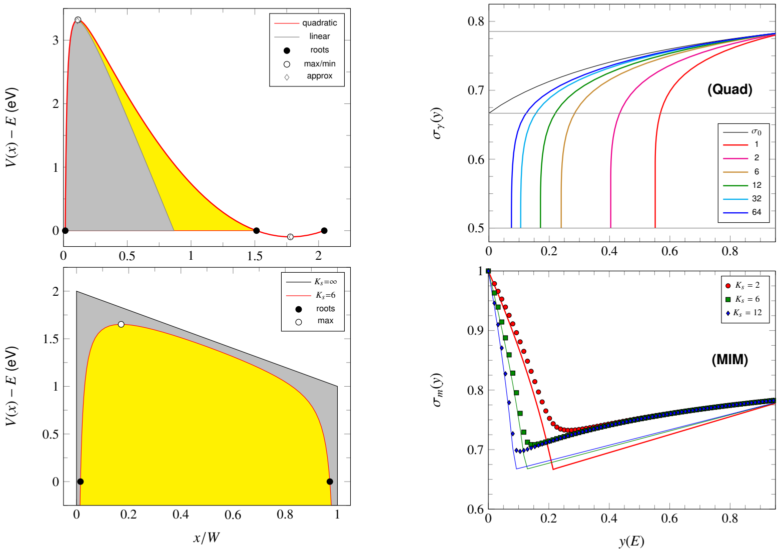

Reflectionless Transmission

Pöschl-Teller (PT) well (sech^2 potential) See Ref. 5

$$V_{pt}(x) = -\frac{\hbar^2 \nu(\nu+1)}{2ma^2}\,\mathrm{sech}^2(x/a) \tag{21}$$

Integer ν, $D(k) \to 1$ = *all* incident e^- for a particular $k = \sqrt{2mE}/\hbar$ are transmitted (yellow)

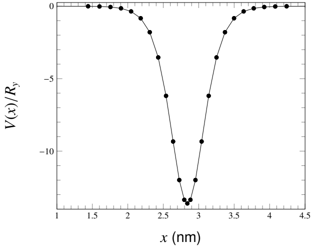

TMA Analysis gives $D(k)$: x_j points shown

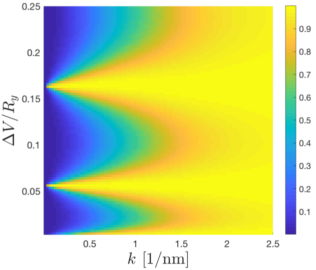

Modify $D_{\triangle}[E(k)]$ (Eq. 2) by k_a and r from fits

$$D(k) \approx \frac{k^r}{\left(k^{2r}+k_a^{2r}\right)^{1/2}} \tag{22}$$

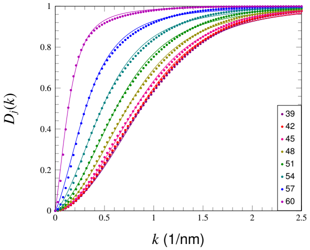

Wave Packet on Delta Barrier

Delta Function Barrier: $V(x) = (\hbar^2 \gamma / 2m)\delta(x)$

Wave function

$$\psi_k(x) = \begin{cases} e^{ikx} + r(k)e^{-ikx} & (x < 0) \\ t(k)e^{ikx} & (x > 0) \end{cases} \quad (23)$$

$$r(k) = -\frac{i\gamma}{2k + i\gamma}; \quad t(k) = \frac{2k}{2k + i\gamma} \quad (24)$$

$$D(k) = |t(k)|^2 = 4k^2/(4k^2 + \gamma^2) \quad (25)$$

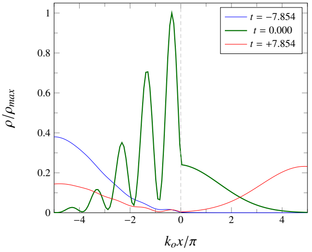

See Ref. 1: Above: gaussian wave packet hitting δ-barrier
Right: $\rho(x,t)$ as contour plot: Horizontal white line $x = 0$
Diagonal white lines = ballistic equations $x_\pm(t) = \pm\hbar k_o t/m$.

Ballistic model (white diagonals): $x(t) = x_o \pm \hbar k t/m$

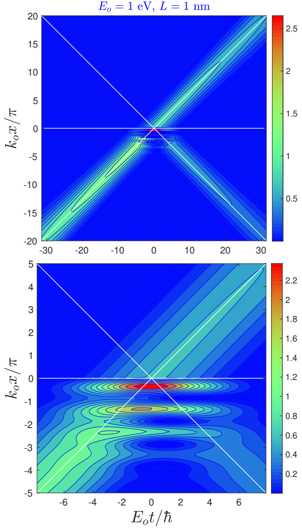

Wave Packet on Wide Rectangular Barrier

- $V(x) = (\hbar^2 k_v^2/2m)\,\Theta(x)\Theta(L_b - x)$
- Group (τ_g), tunneling delay (τ_d), and interference delay (τ_i) times:

$$\begin{aligned} \tau_d(k) &\equiv \left(\frac{m}{\hbar k}\right)\int_0^{L(k)} |\psi_k(k)|^2\,dx \\ \tau_i(k) &\equiv -\frac{\hbar}{k}\Im[r(k)]\left(\frac{dk}{dE}\right) \end{aligned} \qquad (26)$$

- Hartman effect: as $L_b \to \infty$, $\tau_g = \tau_d + \tau_i$ independent of L_b ($\theta \to \infty$)

$$\begin{aligned} \frac{\tau_d(k)}{\tau_o} &= \frac{k}{\kappa(k)}\tanh\theta(k) \\ \frac{\tau_i(k)}{\tau_o} &= \frac{\kappa(k)}{k}\tanh\theta(k) \end{aligned} \qquad (27)$$

$\tau_o = \hbar/V_o = 0.658$ fs for $V_o = 1$ eV

- Gamow Factor $\theta(k)$ is

$$\theta(k) = 2L_b\sqrt{k_v^2 - k^2} \equiv 2\,\kappa(k)\,L_b \qquad (28)$$

Right: dots = Eq. (26); lines = Eq. (27)
See Ref. 1

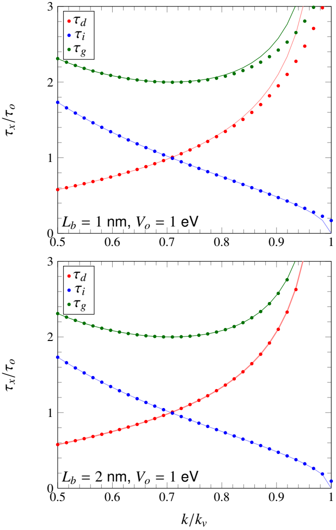

Transmission and Reflection Delay (TARD) Model I

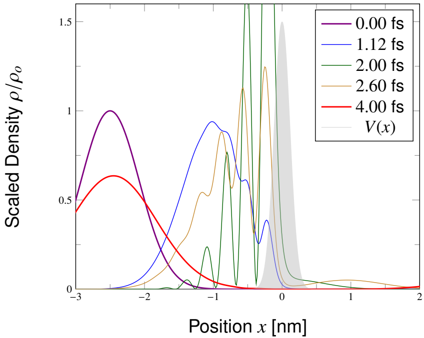

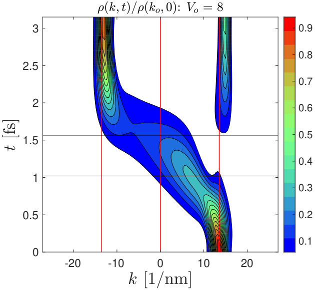

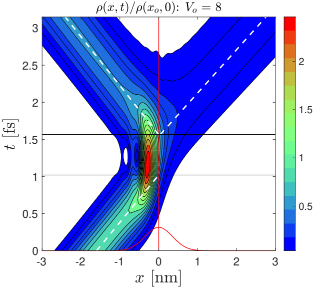

- (*above*) Standard representation of $\rho(x,t)$ for $E_o = 4.5$ eV: transmitted is mostly tunneling. Shaded = $V(x)$. 5 snapshots
- (*right top*) Contour of $\rho(k,t)$: locations of peaks define $k_r = -13.1140$ nm^{-1} and $k_t = 14.8152$ nm^{-1} (TARD k). Vertical red lines are at $k = \pm k_o = \pm 13.5546$ nm^{-1} and $k = 0$.
- (*right bottom*) Contour of $\rho(x,t)$: two horizontal black lines defined by crossings at $(x = 0)$, separated by $= 0.5461$ fs. This is the TARD time
- See Ref. 3

Rectangular Barrier

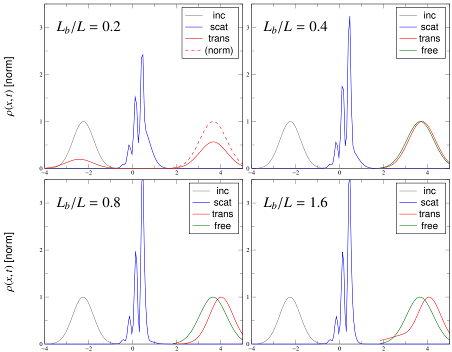

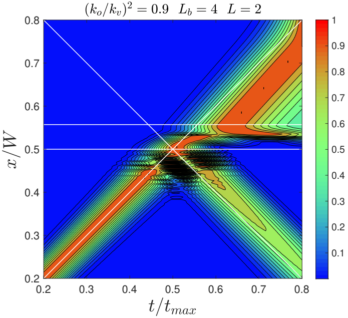

Wave Packets incident on rectangular barrier

Gray and blue lines normalized to incident max. For Case (0.2), solid red line normalized to incident max, and dashed red line to max of transmitted (red) portion; in cases (0.4, 0.8, 1.6), red lines all normalized to transmitted max. Green line is free wave packet normalized to its max, evaluated at the same time as "trans"

$\rho(x, t)$ normalized to max of each t slice

$L = 2$ nm, $L_b = 4$ nm, $E_o = 1$ eV, $E_o/V_o = 0.9$, wave packet incident on rectangular barrier. Delay associated with reflection evident in how contour lines depart from white ballistic lines.

Triangular Barriers

- Propagating gaussian wave packet
- $\rho(x,t)$ norm to each t slice for triangular (Fowler Nordheim) barrier
- horizontal = time, vertical = position
- $F_o = q|\mathcal{E}|$ as shown
- White curved line for $x > x_o = W/2$, where $W = 50$ nm, corresponds to $x_b(t)$
- Both reflected and transmitted show TARD
- Color bar and axis labels $(t/t_{max}, x/W)$ are same as before.

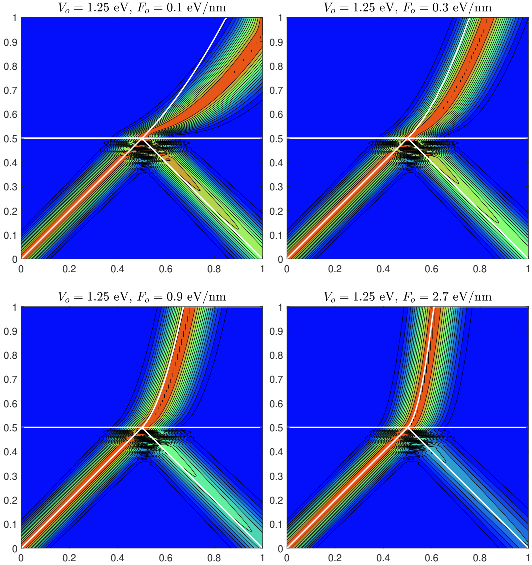

MEAN TRANSVERSE ENERGY FROM ROUGHNESS I

- $F = q|\mathcal{E}|$ is a force: Total force $F^2 = F_x^2 + F_y^2 + F_z^2$ is product of $\beta(x, y, z_s)$ with the background F_o such that $|\vec{F}| = \beta F_o$.
- $\beta(x, y, z_s)$ for surface used to find $|\vec{F}| = \beta F_o$ used in $J_{GTFP}(F, T)$
- $(\beta > 1)$ near apexes of protrusions, $(\beta < 1)$ occurs in valleys between protrusions

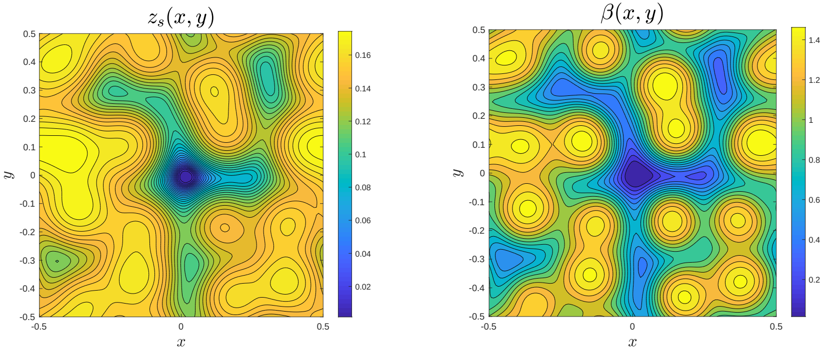

See Ref. 2

Mean Transverse Energy from Roughness II

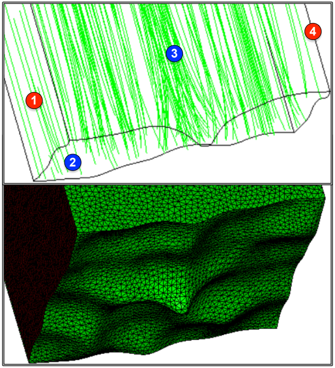

Particle trajectories simulated in MICHELLE
1 in 20 particles are shown.

1. Periodic boundary
2. Cathode with rough surface
3. Vacuum space and trajectories
4. Vacuum space outline (cut at $y = 0$). (*bottom*) Cathode surface showing grid.

Agreement with ballistic impulse approx See Ref. 9

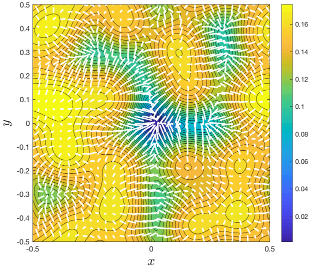

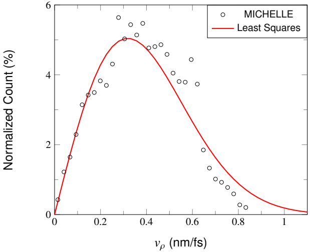

Beam Equation I

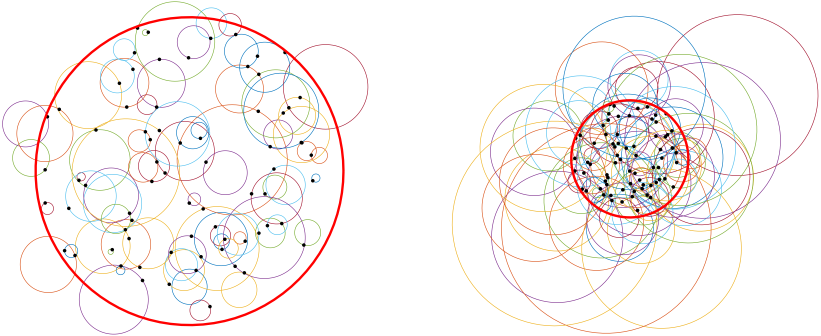

e^- emitted with $\vec{v}_\perp$ rotate about $\vec{B}$ with frequency $\omega_o = qB/m$.

- Cathode boundary: red thick circle. e^- orbit: thin multicolored circles (72 shown) See Ref. 2
- Initial $\vec{v}_\perp$ Maxwell-Boltzmann distributed, randomly placed at black dots
- (*left*) Cathode area is large compared to the orbit radii.
- (*right*) cathode area is comparable to the orbit radii.

Beam Equation II

- Beam radius ≡ RMS average of individual e^- : (x, y) = cathode plane, $\hat{z}$ = beam direction

$$R(t)^2 = \frac{1}{N}\sum_{j=1}^{N}\left[x_j(t)^2 + y_j(t)^2\right] \qquad (29)$$

- $R(t)$ oscillates: $d/dt \rightarrow vd/dz = \beta c d/dz$
  space charge and emittance ε terms added
  Beam Envelope ($\beta, \gamma \leftrightarrow$ relativistic factors)

$$\frac{d^2}{dz^2}R + \left(\frac{qB}{2\beta\gamma mc}\right)^2 R - \frac{2I_a}{(\gamma\beta)^3 I_o}\frac{1}{R} - \frac{\varepsilon^2}{R^3} = 0 \quad (30)$$

- Brillouin flow: blue + green + purple= 0.
  Current density = current over area

$$\frac{I_a}{\pi R^2} = \frac{I_o}{8\pi}\left(\frac{2K_b}{mc^2}\right)^{1/2}\left(\frac{qB}{mc}\right)^2\left\{1 - \frac{8mK_b\varepsilon^2}{q^2B^2R^4}\right\} \qquad (31)$$

$$J_{beam}(\varepsilon) = J_{beam}(0)\{1 - \delta(\varepsilon)\}$$

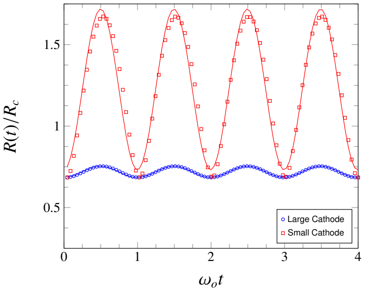

- Symbols: $R(t)$ defined by Eq. (29) for the orbits of prior slide
- Lines: *ad hoc* fit:
  $R_a(t) = R_o - A\cos(6.3\omega_o t)$
- Smaller beam ⇔ more ε affects $J(\varepsilon)$
- See Ref. 2

Concluding Remarks

Model Components

- Accurate Physics demands compete with PIC speed demands
- Optical Parameter Model: Lorentz-Drude for absorption, scattering
- Barrier Transport Model: Analytic Gamow - Shape factor & TMA
- Emission Delay Model: Wave packets via Wigner and Schrodinger
- Roughness models and Intrinsic Emittance
- Effect on Beam Models

Methods

- DFT provides Lorentz-Drude, Barrier parameters, dielectric info
- Emission Studies and TARD: WDF gives unambiguous k_o, suitable for smoothly varying $V(x)$; Schrödinger Eq. gives exact, suitable for abrupt / simple $V(x)$: method of accounting for tunneling/transmission delays in emission is in progress
- Transmission probabilities give launch velocity, current density for PIC